The American Journal of Pathology, Vol. 184, No. 10, October 2014

The American Journal of PATHOLOGY

ajp.amjpathol.org

TUMORIGENESIS AND NEOPLASTIC PROGRESSION

miR-17-92 Cluster Promotes Cholangiocarcinoma Growth

Evidence for PTEN as Downstream Target and IL-6/Stat3 as Upstream Activator

Hanqing Zhu, Chang Han, Dongdong Lu, and Tong Wu

From the Department of Pathology and Laboratory Medicine, Tulane University School of Medicine, New Orleans, Louisiana

Accepted for publication June 6, 2014.

Address correspondence to Tong Wu, M.D., Ph.D., Department of Pathology and Laboratory Medicine, Tulane University School of Medicine, 1430 Tulane Ave, SL-79, New Orleans, LA 70112. E-mail: twu@tulane.edu.

miR-17-92 is an oncogenic miRNA cluster implicated in the development of several cancers; however, it remains unknown whether the miR-17-92 cluster is able to regulate cholangiocarcinogenesis. This study was designed to investigate the biological functions and molecular mechanisms of the miR-17-92 cluster in cholangiocarcinoma. *In situ* hybridization and quantitative RT-PCR analysis showed that the miR-17-92 cluster is highly expressed in human cholangiocarcinoma cells compared with the nonneoplastic biliary epithelial cells. Forced overexpression of the miR-17-92 cluster or its members, miR-92a and miR-19a, in cultured human cholangiocarcinoma cells enhanced tumor cell proliferation, colony formation, and invasiveness, *in vitro*. Overexpression of the miR-17-92 cluster or miR-92a also enhanced cholangiocarcinoma growth *in vivo* in hairless outbred mice with severe combined immunodeficiency (SHO-Prkdc^{scid}Hr^{hr}). The tumor-suppressor, phosphatase and tensin homolog deleted on chromosome 10 (PTEN), was identified as a bona fide target of both miR-92a and miR-19a in cholangiocarcinoma cells via sequence prediction, 3′ untranslated region luciferase activity assay, and Western blot analysis. Accordingly, overexpression of the PTEN open reading frame protein (devoid of 3′ untranslated region) prevented miR-92a— or miR-19a—induced cholangiocarcinoma cell growth. Microarray analysis revealed additional targets of the miR-17-92 cluster in human cholangiocarcinoma cells, including APAF-1 and PRDM2. Moreover, we observed that the expression of the miR-17-92 cluster is regulated by IL-6/Stat3, a key oncogenic signaling pathway pivotal in cholangiocarcinogenesis. Taken together, our findings disclose a novel IL-6/Stat3—miR-17-92 cluster—PTEN signaling axis that is crucial for cholangiocarcinogenesis and tumor progression. *(Am J Pathol 2014, 184: 2828—2839; http://dx.doi.org/10.1016/j.ajpath.2014.06.024)*

miRNAs are a class of small (usually 19 to 24 nucleotides long) noncoding RNAs that globally regulate gene expression through targeting mRNA degradation or translational repression.[1] They are known to target mRNAs through complementary binding at 3′ untranslated regions (UTRs) with their seed sequences (usually two to seven nucleotides).[2,3] Studies in recent years have shown that miRNAs have diverse biological and pathophysiological functions, including regulation of carcinogenesis.[4,5] Although many miRNAs share sequence homology and are grouped into different families, approximately half of human miRNA genes are clustered together.[6–8] The miR-17-92 cluster is one of the cluster miRNAs and has been identified as an oncogene (alias *Oncomir-1*).[9] The miR-17-92 gene (located at the open reading frame of human chromosome 13, *C13orf25*) is expressed as a polycistronic primary transcript containing six tandem stem-loop hairpin structures that ultimately yield six mature miRNAs (miR-17, miR-18, miR-19a, miR-20, miR-19b, and miR-92a). miR-17-92 has been identified as an oncogenic miRNA cluster implicated in several cancers,[10–16] including hepatocellular carcinoma.[17] However, it remains unknown whether the miR-17-92 cluster is involved in cholangiocarcinoma, a highly malignant cancer of the biliary epithelia.

Supported by NIH grants CA102325, CA106280, CA134568, and DK077776 (T.W.).

Disclosures: None declared.

http://dx.doi.org/10.1016/j.ajpath.2014.06.024

Cholangiocarcinoma comprises approximately 10% to 15% of hepatobiliary neoplasms, and its incidence and mortality are increasing.[18–22] The tumor is among the most difficult forms of cancer to treat and generally has a poor prognosis. Most cases are diagnosed at a late stage when lymph node or distant metastasis has occurred and the disease is refractory to treatment. The pathogenesis of cholangiocarcinoma involves activation of growth-promoting signaling pathways and disruption of tumor-suppressor genes. Notably, activation of IL-6/Stat3 signaling and loss of functional phosphatase and tensin homolog deleted on chromosome 10 (PTEN) are among the documented key alterations implicated in cholangiocarcinogenesis.

IL-6 is a classic biliary mitogen that has been shown to increase the growth and survival of biliary epithelial cells and cholangiocarcinoma cells. It mediates actions through binding to gp130 receptor, resulting in phosphorylation and activation of Stat3. Compelling experimental evidences have established a pivotal role of IL-6/Stat3 signaling in cholangiocarcinoma biological features.[23–29] Notably, the serum level of IL-6 in patients with cholangiocarcinoma is significantly elevated, and its level correlates with tumor burden or response to therapy.[30–32]

PTEN is a key tumor-suppressor gene that is disrupted or suppressed in various cancers,[33–36] including cholangiocarcinoma.[37] Although a progressive reduction of PTEN is frequently associated with more aggressive cancers, subtle variations in PTEN levels are recognized to have critical consequences for tumor progression.[34,36] Whereas mutations of *PTEN* have not been reported in cholangiocarcinomas, loss of functional PTEN has been implicated in cholangiocarcinogenesis.[37,38] In a murine model of intrahepatic cholangiocarcinoma, disruption of the *PTEN* gene was associated with development of cholangiocarcinoma.[37] Consistent with the observations that loss of PTEN protein is a prognostic factor in other malignancies, loss of PTEN expression in patients with cholangiocarcinoma has been linked to more aggressive tumor growth parameters and worse survival outcome.[38]

In the current study, we provide the first evidence that the miR-17-92 cluster is highly expressed in cholangiocarcinoma compared with nontumorous biliary epithelial cells. We show that miR-92a is the most abundant miRNA of the miR-17-92 cluster in cholangiocarcinoma. Overexpression of the miR-17-92 cluster or miR-92a enhanced human cholangiocarcinoma cell proliferation, colony formation, and invasiveness *in vitro* and enhanced tumor growth in mice. PTEN was identified as a bona fide target of both miR-92a and miR-19a in cholangiocarcinoma cells. Furthermore, we observed that IL-6/Stat3 enhances the expression of the miR-17-92 cluster in cholangiocarcinoma cells. Our findings suggest a novel interaction among IL-6/Stat3, miR-17-92 cluster, and PTEN signaling pathways in human cholangiocarcinoma cells.

Materials and Methods

Materials

Dulbecco's modified minimum essential medium and heat-inactivated fetal bovine serum (FBS) were purchased from Sigma (St. Louis, MO). OPTI-MEM—reduced serum medium, RPMI 1640 medium, Lipofectamine 2000 reagent, and puromycin were purchased from Invitrogen (Carlsbad, CA). Bronchial Epithelial Cell Basal Medium, with supplemental growth factors in BEGM SingleQuot Kit, was purchased from Lonza (Walkersville, MD). The miR-19a, miR-92a, or miR-17-92 cluster expressed and scrambled control lentiviral particles with enhanced green fluorescent protein were obtained from GeneCopoeia (Rockville, MD). Dulbecco's Phosphate-Buffered Saline Solution was purchased from Thermo Scientific (Logan, UT). Protease inhibitor cocktail and protein phosphatase inhibitor were purchased from Roche (Mannheim, Germany). The Stat3 inhibitor V (Stattic) was purchased from Calbiochem (Darmstadt, Germany). The JAK inhibitors AZD1480 and INCB18424 were purchased from ChemieTek (Indianapolis, IN). Mouse monoclonal anti—β-actin antibody was from Sigma; rabbit anti-PTEN and anti—phospho-Stat3 antibodies were from Cell Signaling (Danvers, MA).

Cell Culture

Four human cholangiocarcinoma cell lines, including CCLP1, SG231, HuCCT1, and TFK1, and one immortalized noncancerous human cholangiocyte cell line (H69) were used. HuCCT1 and TFK1 cells were obtained from the Japanese Cancer Research Resources Bank (Ibaraki City, Japan); H69 cells were kindly provided by Dr. Gregory J. Gores (Mayo Clinic College of Medicine, Rochester, MN). The CCLP1 cells were cultured in Dulbecco's modified minimum essential medium containing 10% FBS, SG231 cells were cultured in OPTI-MEM medium containing 5% FBS, and TFK1 and HuCCT1 cells were cultured in RPMI 1640 medium containing 10% FBS. The H69 cells were cultured in BEBM Basal Medium supplemented with growth factors (BEGM SingleQuot Kit) and 10% FBS. All cells were cultured in a humidified atmosphere of 5% CO_2 incubator at 37°C. The miR-19a, miR-92a, or miR-17-92 cluster—overexpressed and scramble control stable cell lines were established by transduction with the corresponding lentiviral vector or miRNA-scrambled control lentiviral vector, followed by selection with media containing puromycin.

In Situ Hybridization for miRNA

In situ hybridization for miR-92a was performed in the formalin-fixed, paraffin-embedded tissue specimens surgically resected from patients diagnosed with cholangiocarcinoma by using the MiRCURY LNA microRNA ISH Optimization Kit (Exiqon, Vedbaek, Denmark) with the

approval of the Institutional Review Board. Briefly, paraffin sections (6-μm thick) were deparaffinized and treated with 15 μg/mL proteinase-K at 37°C for 10 minutes. After dehydration, slides were incubated with 100 nmol/L miR-92a locked nucleic acid probe (5′-DIG-ACAGGCCGG-GACAAGTGCAATA-3′-DIG) at 50°C for 2 hours. This was followed by stringent washes with 5× standard saline citrate, 1× saline sodium citrate, and 0.2× saline sodium citrate buffers at 50°C; DIG blocking reagent (Roche, Mannheim, Germany) in maleic acid buffer containing 2% sheep serum at room temperature for 15 minutes; and alkaline phosphatase—conjugated anti-digoxigenin (diluted 1:500 in blocking reagent; Roche) at room temperature for 2 hours. Enzymatic development was performed by incubating the slides with 4-nitro-blue tetrazolium and 5-brom-4-chloro-3′-indolylphosphate substrate (Roche) at 30°C for 2 hours to allow formation of dark-blue 4-nitro-blue tetrazolium formazan precipitate, followed by nuclear fast red counterstain (Vector Laboratories, Burlingame, CA) at room temperature for 10 minutes. Slides were then dismantled in water, dehydrated in alcohol solutions, and mounted with mounting medium (Vector Laboratories). Scrambled probe and U6 small nuclear RNA—specific probe were used as system control. A standard 4-point scale method was used to evaluate the staining intensity under microscope and the results were scored as follows: 0 (negative), 1 (+), 2 (++), or 3 (+++), according to established criteria.[39] Specifically, 3 (+++) indicates dark staining that is easily visible with a low-power objective and involves >50% of cells; 2 (++), moderate darkly staining areas and <50% of cells; 1 (+), weak or pale staining in any proportion of cells not easily seen under a low power; and 0 (negative), no staining (showing none of the above staining). The same procedure was used to analyze the cholangiocarcinoma tissue arrays (obtained from BioCat GmbH, Heidelberg, Germany; 44 cases of cholangiocarcinoma and 4 cases of nonneoplastic tissues).

Quantitative RT-PCR

Cellular total RNA was isolated using TRIzol reagent (Invitrogen). Reverse transcription was performed by using an miScript Reverse Transcription Kit (Qiagen, Valencia, CA). miScript SYBR Green PCR Kit (Qiagen) and miScript Primer Assays for six different miRNAs were used to amplify individual mature forms of miR-17/18/19a/19b/20/92a on a C1000 Thermal Cycler (Bio-Rad, Hercules, CA). U6 small nuclear 2 (U6b) was used as the internal control. For quantitation of PTEN mRNA levels, reverse transcription was performed by using the SuperscriptTM II Reverse Transcriptase Kit (Invitrogen). Then, the *PTEN* gene was amplified by using the QuantiFast SYBR Green PCR Kit (Qiagen). Glyceraldehyde-3-phosphate dehydrogenase (GAPDH) was used as the internal control. The GAPDH (Hs_GAPDH_1_SG), PTEN (Hs_PTEN_1_SG), APAF1 (Hs_APAF1_1_SG), and PRDM2 (Hs_PRDM2_1_SG) QuantiTect primers were from Qiagen. The pre—miR-17-92 cluster forward primer is 5′-CAG-TAAAGGTAAGGAGAGCTCAATCTG-3′, and the reverse primer is 5′-CATACAACCACTAAGCTAAAGAATAATC-TGA-3′. miRNA and mRNA expression levels were normalized to their corresponding internal control genes, and relative change was calculated using the $2^{-\Delta\Delta C_T}$ method.

Cell Proliferation WST-1 Assay

The growth of human cholangiocarcinoma cells was measured by using the WST-1 reagent from Roche (Indianapolis, IN). Briefly, 2×10^3 cells were seeded onto each well of 96-well plates and cultured for 24 hours to allow attachment. Then, the medium was replaced with fresh medium containing 1% FBS or specific reagents, as indicated, and the cultures were continued for the indicated days. For cell growth measurement, WST-1 reagent was added to each well and the cells were incubated at 37°C and 5% CO_2 for 1 hour; absorbance at 450 nm was measured using an ELISA plate reader.

Colony-Formation Assay

Cells (1×10^3) were cultured in 10-cm dishes for 14 days to allow colony formation. Colonies were fixed in 100% methanol and stained with 0.1% crystal violet solution (Amersco, Solon, OH) for counting.

Cell Invasion Assay

The cell invasion assay was performed in Matrigel-coated transwell chambers (BD Biosciences Discovery Labware, Bedford, MA). A cell suspension (500 μL; 5×10^4 cells/mL) was added to each of the upper chambers. Cell culture medium containing 10% FBS was added to each of the lower chambers as chemoattractant. After incubating cells at 37°C for 24 hours, the cells on the upper surface of the membrane were removed with a cotton swab. The invading cells on the lower surface of the membrane were fixed in 100% methanol and stained with Mayer's hematoxylin solution (IHC World, Woodstock, MD). Then, the invading cells were counted under a microscope, and for each chamber, eight fields were randomly selected for counting.

Western Blot Analysis

The logarithmically growing cells were washed twice with ice-cold phosphate-buffered saline (PBS), scraped off the plates with 1 mL PBS with 100 nmol/L phenylmethylsulfonyl fluoride, and centrifuged. The cells were then incubated in a lysis buffer containing 50 mmol/L HEPES and 1 mmol/L EDTA (pH 8.0); one tablet of protease inhibitor cocktail (Roche) and one tablet of phosphatase inhibitors (Roche) were added per 10-mL buffer. After sonication on ice, the cell lysates were centrifuged at 12,000 × *g* for 10 minutes at 4°C, and the supernatants were collected for

Western blot analysis. The protein concentration was measured with the Bio-Rad Protein Assay Kit (Bio-Rad, Hercules, CA). After boiling for 5 minutes in the protein loading buffer with 2-mercaptoethanol, the samples were separated on Any kD Mini-PROTEAN TGX Gel (Bio-Rad) and then transferred onto the nitrocellulose membrane (Bio-Rad). The membranes were blocked in PBS with 0.1% Tween 20 (PBS-T) containing 5% nonfat milk for 1 hour at room temperature. Blots were incubated with different primary antibodies (at appropriate dilutions) in PBS-T containing 5% nonfat milk at 4°C overnight. After three washes with PBS-T, the membranes were incubated with IRDye secondary antibody (Licor, Lincoln, NE) at 1:10,000 dilutions in PBS-T containing 5% nonfat milk for 1 hour. After three washes with PBS-T, signals were visualized and the relative densities of protein bands were quantified and normalized to actin using the ODYSSEY Infrared Imaging System (Licor).

miRNA, Anti-miRNA, siRNA, and Plasmid Transfection

siRNA targeting Stat3, GP130, or scrambled control (Ambion, Grand Island, NY), miR-19a mimic or miR-19a–specific anti-miRNA (Qiagen), pcDNA3 control, or pcDNA3-PTEN orf plasmid (Addgene, Cambridge, MA) was transfected into cells by using Lipofectamine 2000 (Invitrogen), as per the manufacturer's instruction. After transfection at indicated time periods, cells were analyzed for proliferation and the cell lysates were obtained for Western blot analysis.

IL-6 and Inhibitor Treatment

Recombinant human IL-6 (R&D Systems, Minneapolis, MN) was prepared according to the product's manual, dissolved in sterile PBS containing 0.1% bovine serum albumin. Stattic, AZD1480, or INCB18424 was dissolved in dimethyl sulfoxide at 10 mmol/L. Serum was withdrawn 24 hours before IL-6 and/or inhibitor treatment to synchronize cells.

DNA Pull-Down Assay

Cells were lysed by sonication in HKMG buffer containing 10 mmol/L HEPES (pH 7.9), 100 mmol/L KCl, 5 mmol/L $MgCl_2$, 10% glycerol, 1 mmol/L dithiothreitol, and 0.5% NP-40 with protease inhibitor cocktail and phosphatase inhibitors for the preparation of nuclear extract. The obtained nuclear extracts were precleared with streptavidin-agarose resin (Thermo Scientific) for 1 hour. The precleared samples were then incubated with 1 μg biotinylated double-stranded oligonucleotide STAT3-binding site (5′-biotin-GTTTCTGA-GAATTCCGGAATTTCCTGAACCAC-3′ and 5′-biotin-GTGGTTCAGGAAATTCCGGAATTCTCAGAAAC-3′; synthesized by Integrated DNA Technologies, Coralville, IA) and 10 μg poly(dI-dC) at 4°C for overnight. DNA-protein complex was collected by incubation with streptavidin-agarose resin on a shaker to prevent precipitation at 4°C for 1 hour. The resin-bound complex was washed at least 5× with 1.0 mL HKMG buffer, followed by centrifugation at 2000 × *g* for 1 to 2 minutes to discard the supernatant. After the resin-bound complex was boiled in SDS-PAGE sample loading buffer, the released protein was loaded onto Any kD Mini-PROTEAN TGX Gel (Bio-Rad) and identified by using Western blot analysis with specific antibodies.

Chromatin Immunoprecipitation

The assay was performed by using a Simplechip Enzymatic Chromatin IP kit (Cell Signaling Technology, Billerica, MA), according to the manufacturer's instructions. Immunoprecipitation was performed by using 5 μg of anti–phospho-STAT3 antibody; rabbit IgG antibody was used as a negative control. Chromatin immunoprecipitation primers were designed to amplify the STAT3 binding region in the miR-17-92 cluster promoter. The primers are as follows: 5′-GGGCATTAAAGACATCCTTTGG-3′ and 5′-GAGCAC-CTCCTTCTTCACATT-3′.

Luciferase Reporter Activity Assay

Cells were seeded in 12-well plates and cultured overnight to allow attachment. The cells were then cotransfected with miRNA mimic or Allstar negative control siRNA (Qiagen) and 0.1 μg per well of pEZX-MT01-PTEN 3′UTR Renilla/firefly dual-luciferase reporter plasmid (GeneCopoeia). The cell lysates were obtained 24 hours after transfection, and luciferase activity was measured in a Centro XS3 LB 960 Microplate Fluorescence Reader (Berthold Technologies, Oak Ridge, TN) by using the Dual-Luciferase reporter assay system (Promega, Madison, WI). The Renilla luciferase activity was used as internal control, and the ratio of Firefly/Renilla activity was calculated for normalization.

mRNA Microarray Analysis

Total RNA from miR-17-92 cluster–overexpressed or control CCLP1 cells were used for Whole Human Genome Oligo Microarray (performed by Arraystar, Rockville, MD). Briefly, total RNA from each sample was amplified and transcribed into fluorescent cRNA using the manufacturer's Agilent's Quick Amp Labeling protocol, version 5.7 (Agilent Technologies, Santa Clara, CA). The labeled cRNAs were hybridized onto the Whole Human Genome Oligo Microarray (4 × 44K; Agilent Technologies). After having washed the slides, the arrays were scanned by the Agilent Scanner G2505B (Agilent Technologies). Agilent Feature Extraction software version 11.0.1.1 (Agilent Technologies) was used to analyze acquired array images. Quantile normalization and subsequent data processing were performed using the GeneSpring GX software version 11.5.1 (Agilent Technologies). Raw data of detected genes were normalized for further analysis. Differentially expressed genes were

identified through fold change filtering. The data were deposited into Gene Expression Omnibus (*http://www.ncbi.nlm.nih.gov/geo*; accession number GSE58060).

SCID Mice Tumor Xenograft Studies

Four-week-old male severe combined immunodeficiency (SCID) hairless outbred (SHO) mice (Crl:SHO-*Prkdc*^{scid}*Hr*^{hr}, strain 474) were purchased from Charles River (Wilmington, MA). Two complementary xenograft models (s.c. and orthotopic) were used. For the s.c. xenograft model, 3×10^6 miR-92a− or miR-17-92 cluster−overexpressed or control CCLP1 cells were inoculated into the flanks of mice (six mice per group), and the mice were observed over 4 weeks for tumor formation. The tumor volume was measured weekly with a caliper and calculated by using the following formula: larger diameter $\times$ (smaller diameter)$^2/2$. On sacrifice, the tumors were recovered and the wet weights of each tumor were determined. A portion of each tumor was selected for H&E staining, Western blot analysis, and quantitative RT-PCR (RT-qPCR) analysis. For the orthotopic transplant model, 3×10^7/mL miR-17-92 cluster−overexpressed or control CCLP1 cell suspension was mixed with Corning Matrigel Basement Membrane Matrix High Concentration (Corning, NY) in a 1:1 ratio; a 50-μL final volume (containing 7.5×10^5 cells) was injected directly into the liver of mice in surgery under local anesthesia. The mice were sacrificed 6 weeks after intrahepatic inoculation to document tumor growth.

Statistical Analysis

Results are presented as means ± SD or SEM from a minimum of three replicates. Differences between groups were compared using either Student's *t*-test or one-way analysis of variance. $P < 0.05$ was considered statistically significant. The analysis was performed using SPSS statistical software version 19.0 (IBM, Armonk, NY). For data from human samples, statistical significance between means was determined by the nonparametric Kruskal-Wallis test.

Results

Expression of miR-92a Is Increased in Human Cholangiocarcinoma Tissues and Cell Lines

The miR-17-92 cluster is a polycistronic primary transcript and yields six mature miRNAs: miR-17, miR-18a, miR-19a, miR-20a, miR-19b, and miR-92a (Figure 1A). To determine the

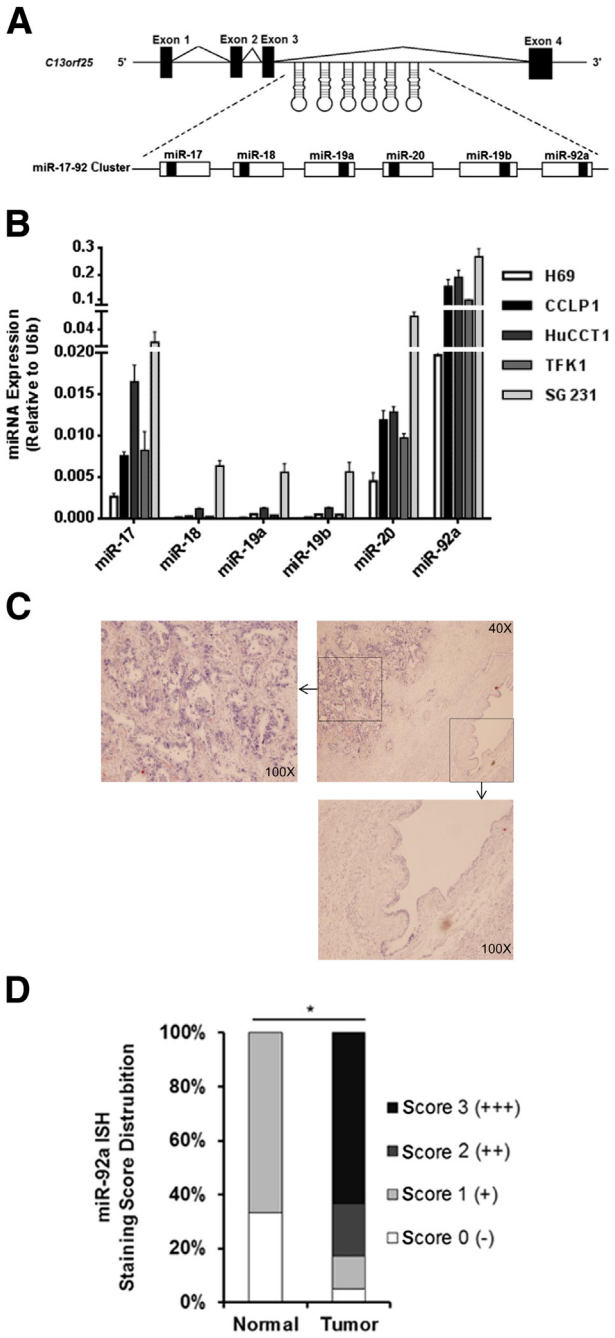

Figure 1 High expression of the miR-17-92 cluster in human cholangiocarcinoma tissues and cell lines. **A:** Genomic structure of the miR-17-92 cluster. The miR-17-92 cluster is polycistronic, and located at *C13orf25*. The pre−miR-17-92 cluster is cleaved, generating six mature miRNAs (miR-17, miR-18, miR-19a, miR-20, miR-19b, and miR-92). **B:** Expression of the miR-17-92 cluster in cholangiocarcinoma cell lines. RT-qPCR for mature miRNA in the miR-17-92 cluster in a human transformed cholangiocyte cell line (H69) and four human cholangiocarcinoma cell lines (CCLP1, HuCCT1, SG231, and TFK1). Total cellular RNA was extracted for RT-qPCR ($n = 3$). The expression level of each individual miRNA is normalized to RNU6B (internal control). All of the six miRNAs (miR-17/18/19a/19b/20/92) are highly expressed in four cholangiocarcinoma cell lines (CCLP-1, HuCCT1, SG231, and TFK-1 cells) compared with the noncancerous control cell line H69. Among the six mature miRNAs, miR-92a is the most abundant, followed by miR-17 and miR-20. **C:** *In situ* hybridization for mature miR-92a in human cholangiocarcinoma tissues. Representative *in situ* hybridization images depict the expression of miR-92a in human cholangiocarcinoma tissues. Note positive miR-92a staining in cholangiocarcinoma cells and negative staining in normal bile duct epithelial cells (positive signals are in dark blue; nuclei were counterstained in red). **D:** Distribution of miR-92a staining intensity scores in human cholangiocarcinoma tissue arrays ($N = 44$). *$P < 0.05$ (Kruskal-Wallis nonparameter test).

expression patterns of these six miRNAs, we measured their levels by RT-qPCR analyses in human cholangiocarcinoma cells and noncancerous human biliary epithelial cells. Higher levels of miR-92a, miR-20, and miR-17 expression were observed in all four human cholangiocarcinoma cell lines (CCLP1, HuCCT1, SG231, and TFK1) when compared with the noncancerous human biliary epithelial cell line (H69) (Figure 1B). The expression levels of miR-18, miR-19a, and miR-19b were also increased in cholangiocarcinoma cells (noticeably increased in SG231 cells and slightly increased in HuCCT1, CCLP1, and TFK1 cells). miR-92a is the highest among all of the six miRNAs of the cluster in all four human cholangiocarcinoma cell lines.

Given that miR-92a is the most abundant miRNA among the miR-17-92 cluster in human cholangiocarcinoma cell lines, we performed *in situ* hybridization using locked nucleic acid–modified probe against miR-92a in human cholangiocarcinoma tissue samples and nonneoplastic bile duct epithelia. Formalin-fixed, paraffin-embedded tumor and liver tissues from 12 patients who underwent surgical resections for cholangiocarcinoma and 41 cases of cholangiocarcinoma tissue arrays were analyzed. We observed that miR-92a is highly expressed in 12 (100%) of 12 cases of archived cholangiocarcinoma tissues, which is in contrast to the weak or absent staining in nonneoplastic bile duct and peribiliary glands (Figure 1C). For cholangiocarcinoma tissue array analysis, the staining frequency and intensity of miR-92a are also significantly higher in cholangiocarcinoma cells (63.41% +++, 19.51% ++, 12.20% +, and 4.88% −) compared with the nonneoplastic bile duct epithelial cells (0.0% +++, 0.0% ++, 66.67% +, and 33.33% −; $P = 0.04$) (Figure 1D and Supplemental Table S1). These findings document increased expression of the miR-17-92 cluster, particularly miR-92a, in human cholangiocarcinoma tissues and cell lines.

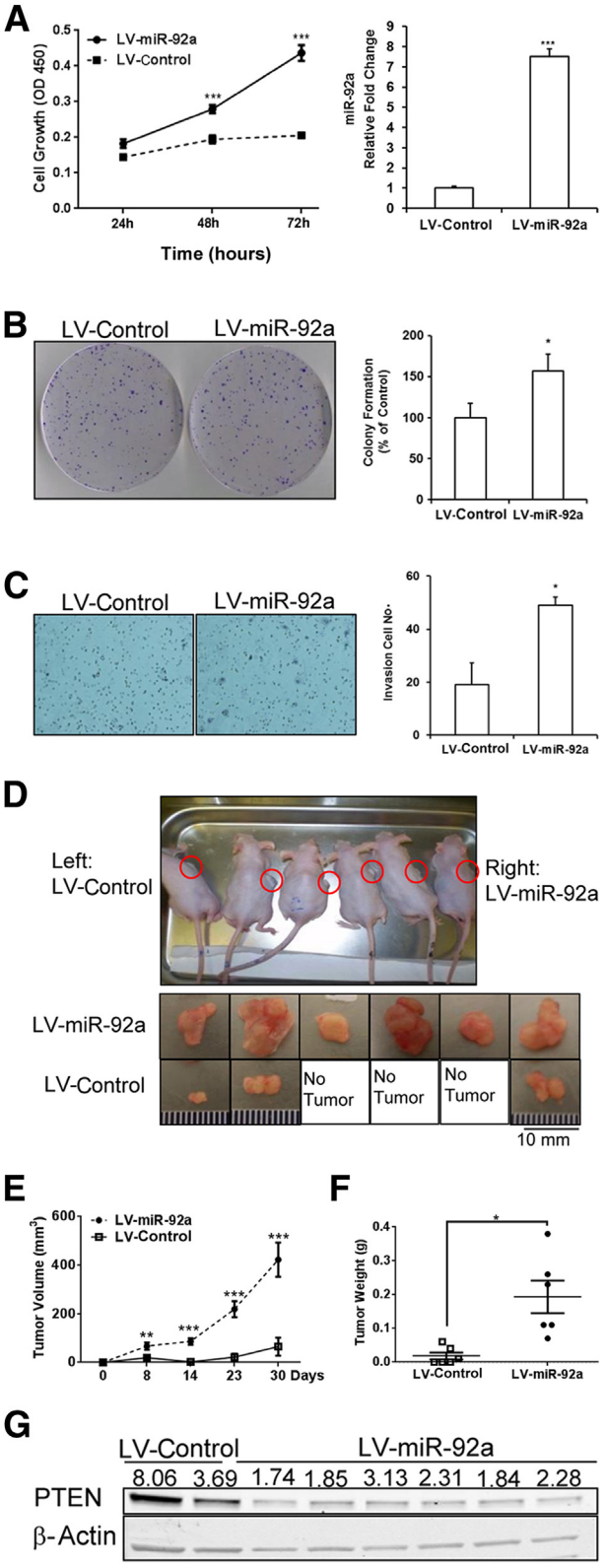

Figure 2 miR-92a overexpression promotes cholangiocarcinoma cell growth *in vitro* and *in vivo*. **A–C:** miR-92a overexpression promotes cholangiocarcinoma cell growth, colony formation, and cell invasion *in vitro*. Human cholangiocarcinoma cells (CCLP1) were infected with miR-92a lentivirus and miRNA scrambled control lentivirus, respectively. The stably transduced cells were analyzed for proliferation, colonogenic potential, and invasion ability, as described in *Materials and Methods*. **A:** miR-92a overexpression promotes cholangiocarcinoma cell growth. Cell growth curves of human cholangiocarcinoma cells (CCLP1) stably transduced with miR-92a lentivirus (indicated as LV-miR-92a) or scrambled control (indicated as LV-control). miR-92a levels were measured by RT-qPCR. **B:** miR-92a overexpression enhances cholangiocarcinoma cell colony formation. The numbers of colonies were counted after 14 days. Representative images showing colonies formed in cell culture dishes. Average colony formation efficiency is shown. **C:** miR-92a overexpression promotes cholangiocarcinoma cell invasion. Representative images showing migrated cell staining by hematoxylin. Average numbers of the invaded cells are shown. **D–G:** miR-92a promotes cholangiocarcinoma growth *in vivo*. miR-92a–overexpressed or scrambled control CCLP1 cells (1.0×10^8) were inoculated s.c. into flank areas of SCID hairless mice ($n = 6$), and the mice were closely monitored for tumor growth. Thirty days after inoculation, the mice were sacrificed and the tumors were recovered. **D:** Photographs of xenograft tumor masses from SCID mice highlight that miR-92a promotes tumor growth. Images are of the mice and the xenograft tumors that were recovered. **E:** miR-92a overexpression significantly increases xenograft tumor volume. **F:** miR-92a significantly increases the weight of the xenograft tumors. **G:** Western blot analysis reveals decreased PTEN protein levels in xenograft tumor tissues by miR-92a. Data are presented as means ± SEM (**A–C**) or means ± SD (**E** and **F**). $N = 3$ (**A–C**); $N = 6$ (**E** and **F**). $^*P < 0.05$, $^{**}P < 0.01$, and $^{***}P < 0.001$.

miR-92a Enhances Cholangiocarcinoma Cell Growth, *in Vitro* and *in Vivo*

To investigate the role of miR-92a in cholangiocarcinoma cell growth, we constructed human cholangiocarcinoma cell lines with stable overexpression of miR-92a by infecting the parental cell line (CCLP1) with lentivirus particles carrying the miR-92a gene (this vector also carries the enhanced green fluorescent protein gene under the control of the same promoter). High infection efficiency was confirmed by the expression of enhanced green fluorescent protein in nearly all transduced cells. Successful overexpression of miR-92a in miR-92a lentivirus stably transduced cells was verified by RT-qPCR (cells transduced with lentivirus carrying scrambled control miRNA were used as control). Overexpression of miR-92a significantly increased the growth of cholangiocarcinoma cells *in vitro* (Figure 2A). miR-92a overexpression also increased colony-formation efficiency and enhanced cell invasion (Figure 2, B and C). These findings demonstrate that miR-92a increases the malignant potential of cholangiocarcinoma cells *in vitro*.

To determine the effect of miR-92a on cholangiocarcinoma growth *in vivo*, we inoculated miR-92a—overexpressed and scrambled control CCLP1 cells into the flanks of SCID hairless outbred mice (SHO-Prkdc^{scid}Hr^{hr}). Although only three of six mice inoculated with scrambled control cells showed visible tumors, six of six mice inoculated with miR-92a overexpression cells developed visible tumors 30 days after inoculation (Figure 2D). The scrambled control tumors were smaller ($P < 0.05$) and lower in weight compared with the miR-92a—overexpressed tumors (Figure 2, D and E). An approximately sixfold increase in tumor weight was observed in miR-92a—overexpressed tumors compared with the controls (0.19 ± 0.04 g versus 0.02 ± 0.01 g; $P = 0.014$) (Figure 2F). Western blot analysis of the tumor tissues showed reduction of PTEN protein in miR-92a—overexpressed tumors (Figure 2G).

miR-17-92 Cluster Increases Cholangiocarcinoma Cell Growth, *in Vitro* and *in Vivo*

Given that miR-92a is able to increase cholangiocarcinoma cell growth, as shown above, we sought to further evaluate

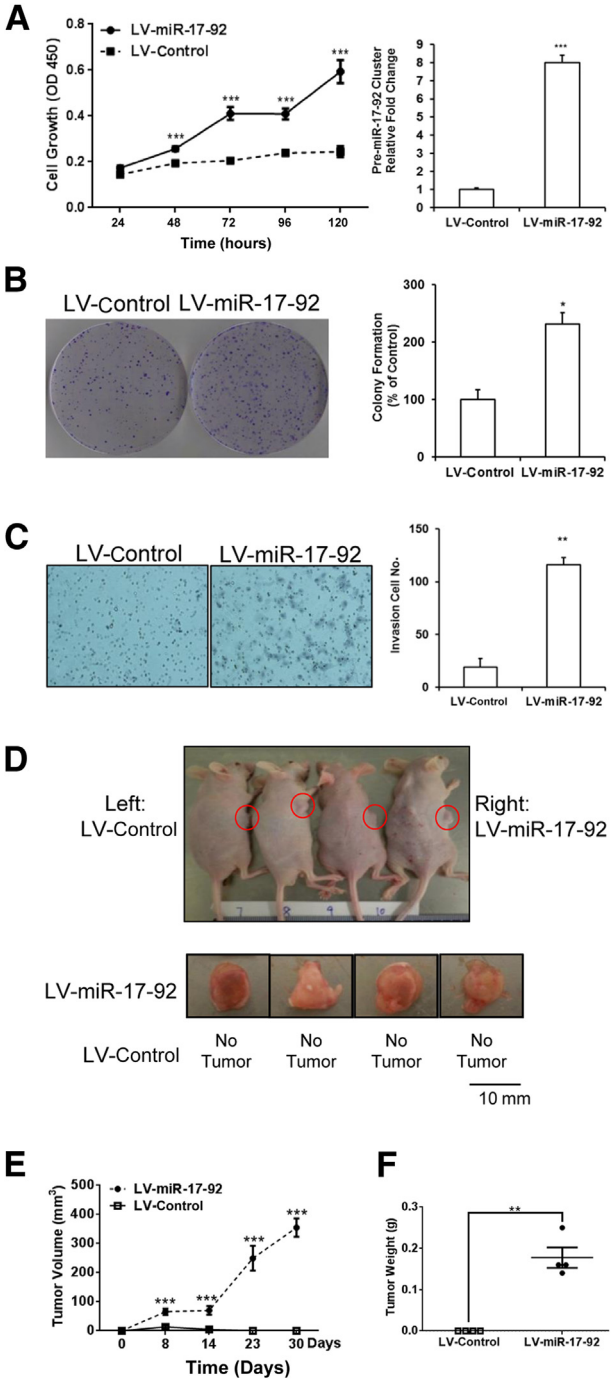

Figure 3 Overexpression of miR-17-92 cluster promotes cholangiocarcinoma cell growth *in vitro* and *in vivo*. The miR-17-92 cluster promotes human cholangiocarcinoma cell proliferation (**A**), colony formation (**B**), and cell invasion (**C**) *in vitro*. Human cholangiocarcinoma cells (CCLP1) were infected with miR-17-92 cluster lentivirus and miRNA scrambled control lentivirus, respectively, and the stable cells were analyzed for proliferation, colonogenic potential, and invasion ability, as described in *Materials and Methods*. **A:** Cell proliferation assay (WST-1). Cell growth curves of human cholangiocarcinoma cells (CCLP1) stably transduced with miR-17-92 cluster lentivirus (indicated as LV-miR-17-92) or scrambled control LV-control. The miR-17-92 cluster promotes cell growth in cholangiocarcinoma cell lines. Pre—miR-17-92 cluster levels were measured by RT-qPCR. **B:** miR-17-92 cluster overexpression enhances cholangiocarcinoma cell colony formation. The numbers of colonies were counted after 14 days. Representative images show colonies formed in cell culture dishes. Average colony-forming efficiency is shown. **C:** miR-17-92 cluster overexpression promotes cholangiocarcinoma cell invasion. Representative images show migrated cell staining by hematoxylin. Average numbers of invaded cells are shown. **D—F:** The miR-17-92 cluster promotes cholangiocarcinoma growth *in vivo*. miR-17-92 cluster—overexpressed or scrambled control CCLP1 cells (1.0×10^8) were inoculated s.c. into flank areas of SCID hairless mice ($n = 6$), and the mice were closely monitored for tumor growth. Thirty days after inoculation, the mice were sacrificed and the tumors were recovered. **D:** Photographs of xenograft tumor masses from SCID mice show that the miR-17-92 cluster promotes tumor growth. **E:** The volume of xenograft tumors is significantly increased by miR-17-92 cluster overexpression. **F:** The weight of xenograft tumors is significantly increased by miR-17-92 cluster overexpression. Data are from four SCID mice (two mice died before 30 days). Data represent means ± SEM (**A**—**C**) or means ± SD (**E** and **F**). $N = 3$ (**A**—**C**); $N = 4$ to 6 (**E**); $N = 4$ (**F**). $^*P < 0.05$, $^{**}P < 0.01$, and $^{***}P < 0.001$.

the effect of the miR-17-92 cluster by stably transducing cholangiocarcinoma cells with lentivirus particles expressing miR-17-92 cluster or the scrambled control miRNA. Overexpression of the miR-17-92 cluster significantly increased the cholangiocarcinoma cell growth *in vitro* (Figure 3A). miR-17-92 overexpression also increased colony-formation efficiency and enhanced cell invasion (Figure 3, B and C). When these cells were inoculated s.c. into SCID hairless mice (SHO-Prkdc^{scid}Hr^{hr}), the miR-17-92 cluster–overexpressed cells produced visible tumors 30 days after inoculation; in contrast, the scrambled control cells failed to produce any tumor under the same condition (Figure 3, D–F). When these cells were transplanted orthotopically into the livers of SCID hairless mice, the miR-17-92 cluster–overexpressed tumors exhibited larger tumor volume compared with the scrambled control tumors (Supplemental Figure S1). These findings provide *in vitro* and *in vivo* evidences for a tumor-promoting effect of the miR-17-92 cluster in cholangiocarcinoma.

Because miR-19a is another member of the miR-17-92 cluster implicated in the growth regulation of other cancer cells,[40] we performed further experiments to determine whether miR-19a might play a role in human cholangiocarcinoma cells. Overexpression of miR-19a enhanced cholangiocarcinoma cell proliferation, colony formation, and cell invasion (Figure 4A). Collectively, our findings document an important oncogenic role of the miR-17-92 cluster and its members (including miR-92a and miR-19a) in cholangiocarcinoma cell growth.

PTEN Is a Direct Target of miR-92a and miR-19a in Cholangiocarcinoma Cells

In an effort to identify the potential targets that mediate miR-17-92 actions in cholangiocarcinoma cells, we used the online prediction tool Miranda (*http://www.microrna.org/microrna*, last accessed October 12, 2013). This approach led to identification of PTEN as a key downstream target. Complementary sequences of miR-92a and miR-19a were identified in the 3′UTR of PTEN mRNA (Figure 5A). RT-qPCR and Western blot analyses showed that overexpression of the miR-17-92 cluster or its members (miR-92a or miR-19a) led to reduction of PTEN mRNA and protein levels (Figure 5, B and C). Treatment of human cholangiocarcinoma cells with miR-92a or miR-19a mimic also reduced PTEN expression (Figure 5C). Accordingly, miR-92a or miR-19a mimic treatment decreased the PTEN 3′UTR luciferase reporter activity (Figure 5D). The role of PTEN in miR-92a– and miR-19a–induced cholangiocarcinoma cell growth was further supported by the observation that forced overexpression of PTEN open reading frame protein (without the 3′UTR) partially prevented miR-92a– and miR-19a–induced tumor cell growth (Figure 5E). These results demonstrate that PTEN is a direct target of the miR-17-92 cluster through two of its members, miR-92a and miR-19a.

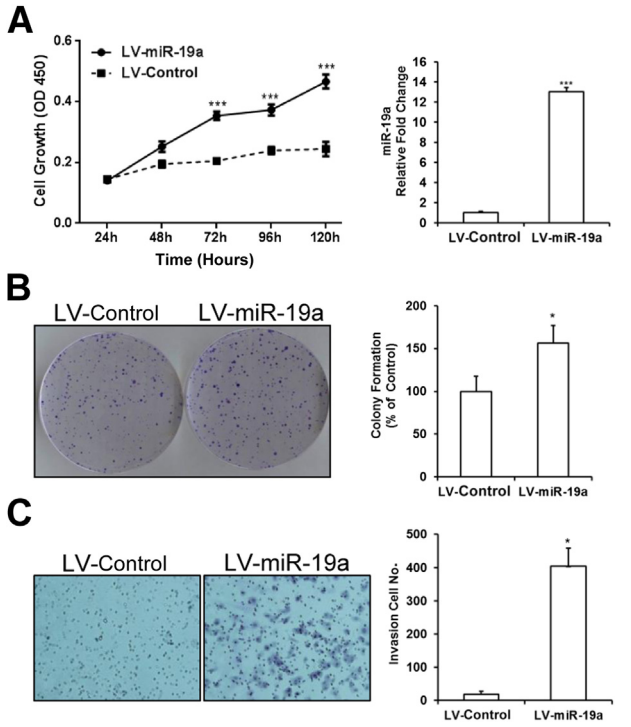

Figure 4 miR-19a overexpression promotes cholangiocarcinoma cell growth and colony formation *in vitro*. **A:** miR-19a overexpression promotes cholangiocarcinoma cell growth. Cell growth curves of human cholangiocarcinoma cells (CCLP1) stably transduced with miR-19a lentivirus (indicated as LV-miR-19a) or scrambled control (indicated as LV-control). miR-19a levels were measured by RT-qPCR. **B:** miR-19a overexpression promotes cholangiocarcinoma cell colony formation. The numbers of colonies were counted after 14 days. Representative images show colonies formed in cell culture dishes. Average colony formation efficiency is shown. **C:** miR-19a overexpression promotes cholangiocarcinoma cell invasion. Representative images show migrated cell staining by hematoxylin. Average numbers of invaded cells are shown. Data are presented as means ± SEM. $N = 3$. $^{*}P < 0.05$, $^{***}P < 0.001$.

Transcriptome and Sequence Analyses for Additional Targets of miR-17-92 Cluster

To predict other targets of the miR-17-92 cluster, we performed sequence analysis by using TargetScan (*http://www.targetscan.org*, last accessed October 12, 2013), PicTar (*http://pictar.mdc-berlin.de*, last accessed October 12, 2013), and Miranda. Such sequence analysis predicted >30,000 targets that have at least one binding site for one or multiple miRNAs in the miR-17-92 cluster. As a parallel approach, we performed transcriptome analysis using mRNA microarray and found that 2861 genes were down-regulated in miR-17-92 cluster–overexpressed cells compared with scrambled control cells (Supplemental Figure S2A). There were 960 common genes identified by both sequence prediction and transcription analysis. PANTHER pathway analysis (*http://www.pantherdb.org*, last accessed October 12, 2013) indicates that these common genes are most enriched in Wnt, cadherin, and inflammation pathways (Supplemental Table S2), which is consistent with the molecular features of cholangiocarcinoma.[41] By

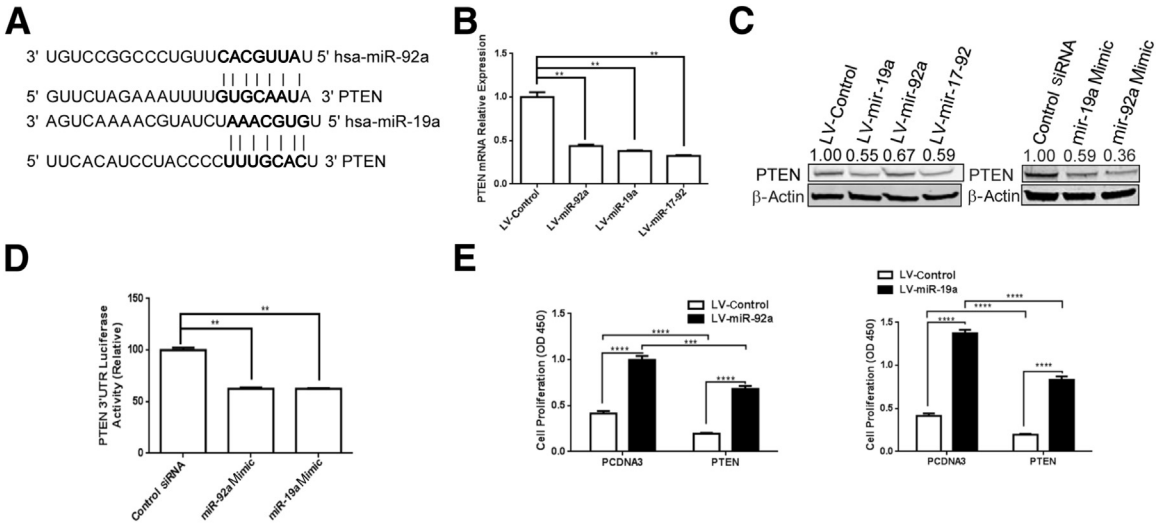

Figure 5 miR-17-92 targets PTEN via miR-92a and miR-19a in cholangiocarcinoma cells. **A:** Predicted 8-mer and 7-mer-m8 binding sequence for miR-92a and miR-19a in the 3′UTR of PTEN mRNA. **B:** PTEN mRNA levels are decreased in miR-19a, miR-92a, or miR-17-92 cluster—overexpressed cells, as determined by RT-qPCR analysis. **C:** PTEN protein levels are down-regulated in miR-19a, miR-92a, and miR-17-92 cluster—overexpressed stable cell lines, as determined by using Western blot analysis. PTEN protein levels are also down-regulated by miR-19a mimic or miR-92a mimic in CCLP-1 cells. **D:** miR-92a or miR-19a mimic significantly reduces PTEN 3′UTR luciferase activity. CCLP1 cells were transfected with miRNA mimic or scrambled control, together with PTEN 3′UTR dual-luciferase reporter plasmid. The luciferase activity was analyzed 24 hours after transfection. **E:** PTEN (ORF) overexpression inhibits the cell growth induced by miR-19a or miR-92a. Data are presented as means ± SEM (**B** and **E**) or means ± SD (**D**). $N = 3$ (**B** and **D**); $N = 6$ (**E**). $^{**}P < 0.01$, $^{***}P < 0.001$, and $^{****}P < 0.0001$.

comparing the miR-17-92 cluster—down-regulated genes with the online database of human tumor-suppressor gene,[42] we found several highly possible targets, including APAF-1 and PRDM2, in addition to PTEN, which are significantly down-regulated in miR-17-92 cluster—overexpressed cholangiocarcinoma cells (Supplemental Table S3 and Supplemental Figure S2B). These findings suggest that miR-17-92—regulated cholangiocarcinoma growth may also involve additional targets (including APAF-1 and PRDM2, among others).

The Expression of miR-17-92 Cluster Is Up-Regulated by IL-6/Stat3 Signaling

Given the noticeable up-regulation of miR-17-92 cluster in cholangiocarcinoma cells, we sought to further explore the mechanism that regulates miR-17-92 expression in cholangiocarcinoma cells. Because the promoter region of the miR-17-92 cluster gene contains a conserved binding site for Stat3[43,44] (Figure 6D), we postulated that activation of IL-6/Stat3 signaling might be a potential mechanism for miR-17-92 cluster up-regulation during cholangiocarcinogenesis. Indeed, treatment of human cholangiocarcinoma cells with IL-6 significantly increased the expression of pre—miR-17-92 cluster mRNA (Figure 6A). IL-6 treatment also significantly increased the levels of each individual mature miRNA of the miR-17-92 cluster (by 77- to 250-folds) (Supplemental Figure S3). IL-6—mediated induction of pre—miR-17-92 cluster mRNA was almost completely abolished by siRNA knockdown of Stat3 or GP130 ($P < 0.01$) (Figure 6B). Similarly, pretreatment of human cholangiocarcinoma cells with 20 μmol/L Stat3 phosphorylation inhibitor Stattic[45] or 20 μmol/L JAK inhibitor (AZD1480 or INCB18424) also abolished IL-6—induced up-regulation of the miR-17-92 cluster (Figure 6, C and D). The DNA pull-down assay and the chromatin immunoprecipitation assay showed that IL-6 treatment increased the association of phosphorylated Stat3 to its DNA binding site in miR-17-92 cluster gene promoter (Figure 6, E and F). These findings suggest an important role of IL-6/Stat3 signaling for up-regulation of the miR-17-92 cluster in human cholangiocarcinoma cells.

Discussion

The current study provides the first evidence that the miR-17-92 cluster is highly expressed in human cholangiocarcinoma cells compared with the noncancerous human biliary epithelial cells. Our data show that miR-92a is the most abundant miRNA among the six mature miRNAs of the miR-17-92 cluster in human cholangiocarcinoma. The role of the miR-17-92 cluster in cholangiocarcinoma growth is established by complementary *in vitro* and *in vivo* studies. We observed that forced overexpression of the miR-17-92 cluster or its members, miR-92a and miR-19a, in cultured human cholangiocarcinoma cells enhanced tumor cell proliferation, colony formation, and invasiveness *in vitro*. Overexpression of the miR-17-92 cluster or miR-92a was also found to enhance xenograft cholangiocarcinoma growth in mice. These findings establish a key tumor-promoting role of the miR-17-92 cluster in cholangiocarcinoma (Figure 7).

Our data show that PTEN is a direct target of the miR-17-92 cluster through two of its members, miR-92a and

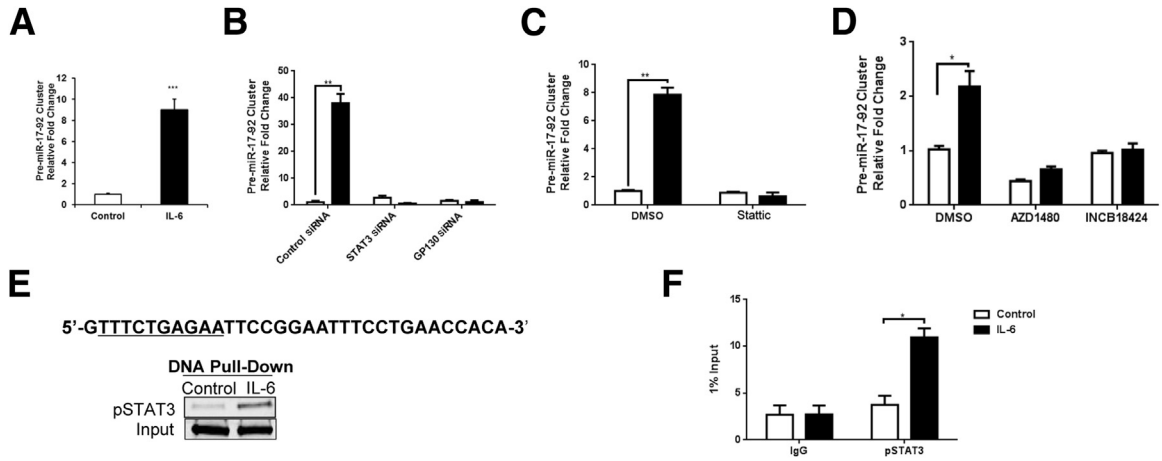

Figure 6 IL-6 up-regulates miR-17-92 expression in cholangiocarcinoma cells through Stat3 activation. **A:** Stimulation of CCLP-1 cells with 20 ng/mL IL-6 increases the expression of the pre—miR-17-92 cluster, as determined by RT-qPCR. **B:** IL-6—mediated induction of the pre—miR-17-92 cluster is abolished by siRNA knockdown of Stat3 or the IL-6 receptor, GP130. RT-qPCR data are presented. **C:** IL-6—mediated induction of the pre—miR-17-92 cluster is abolished by 20 μmol/L Stat3 phosphorylation inhibitor Stattic. RT-qPCR data are presented. **D:** IL-6—mediated induction of the pre—miR-17-92 cluster is abrogated by 20 μmol/L JAK inhibitor, AZD1480 or INCB18424. RT-qPCR data are presented. **E:** IL-6 treatment increases binding of activated Stat3 to the promoter region of the miR-17-92 cluster, as determined by biotinylated oligonucleotide precipitation assay. Stat3 binding sequence at promoter region of pre—miR-17-92 was biotinylated-linked and used to precipitate proteins after 20 ng/mL IL-6 treatment for 1 hour. Phospho-Stat3 protein was detected by using Western blot analysis. **F:** Chromatin immunoprecipitation assay. The chromatin extracted from CCLP1 cells, treated with IL-6 or control vehicle, was subjected to immunoprecipitation with phospho-STAT3 antibody, and the precipitates were subjected to RT-qPCR analysis using primers to amplify the STAT3 binding region. Normal rabbit IgG was used as the negative control. RT-qPCR data are presented. Data are presented as means ± SEM (**A**—**D** and **F**). $N = 3$ (**A**—**D** and **F**). $^{*}P < 0.05$, $^{**}P < 0.01$, and $^{***}P < 0.001$.

miR-19a. This assertion is based on the following observations: i) complementary sequences of miR-92a and miR-19a are present in the 3′UTR of PTEN mRNA, ii) overexpression of the miR-17-92 cluster or its members (miR-92a or miR-19a) decreased PTEN mRNA and protein levels in human cholangiocarcinoma cells, iii) treatment of human cholangiocarcinoma cells with miR-92a or miR-19a reduced PTEN protein expression, and iv) miR-92a or miR-19a mimic treatment decreased PTEN 3′UTR luciferase reporter activity in human cholangiocarcinoma cells. Therefore, inhibition of PTEN may represent an important mechanism for miR-17-92 cluster—mediated cholangiocarcinoma growth. The involvement of PTEN in miR-17-92—induced cholangiocarcinoma cell growth is further supported by the observation that overexpression of PTEN open reading frame protein prevented miR-92a— or miR-19a—induced tumor cell growth.

In addition to PTEN, we observe that miR-17-92 cluster also targets other proteins, including APAF-1 and PRDM2, in human cholangiocarcinoma cells. It is possible that these additional targets may also be implicated in miR-17-92—mediated cholangiocarcinoma growth.

Herein, we show that IL-6/Stat3 signaling transcriptionally regulates the expression of the miR-17-92 cluster in cholangiocarcinoma cells. This assertion is based on the following observations: i) a conserved Stat3 binding site is present in the miR-17-92 cluster gene promoter, ii) IL-6 treatment increased the levels of pre—miR-17-92 and mature miRNAs of the miR-17-92 cluster, iii) siRNA knockdown of Stat3 or GP130 or inhibition of Stat3 phosphorylation abolished IL-6—induced induction of the pre—miR-17-92 cluster, and iv) IL-6 treatment increased the association of phosphorylated Stat3 to its DNA binding site in the miR-17-92 cluster gene promoter. Thus, activation of IL-6/Stat3 signaling may be an important factor for induction of miR-17-92 expression in cholangiocarcinoma.

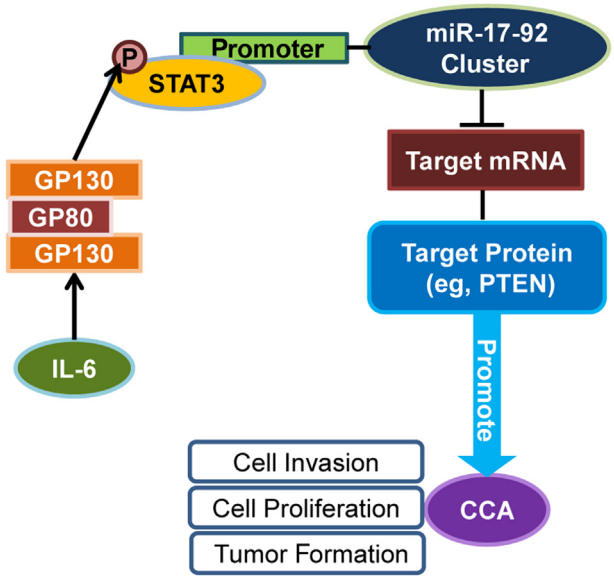

Figure 7 Schematic illustration of the proposed mechanism for miR-17-92 cluster—induced cholangiocarcinoma growth. The miR-17-92 cluster can directly target PTEN via miR-19a and miR-92, which associate with 3′UTR of PTEN. Reduction of PTEN enhances cholangiocarcinoma cell proliferation and invasion *in vitro* and tumor formation *in vivo*. Furthermore, IL-6 can up-regulate the expression of miR-17-92 cluster through Stat3-mediated transcription of the pre—miR-17-92 cluster. CCA, cholangiocarcinoma.

In this context, it is notable that recent studies have shown that miR-17-92 targets JAK-STAT pathway inhibitor SOCS3 (suppressors of cytokine signaling)[46] and PIAS3 (protein inhibitor of activated Stat3),[47] two key negative regulators of the JAK-STAT pathway. Thus, it is possible that the IL-6/Stat3−induced miR-17-92 cluster may further amplify IL-6/Stat3 signaling through targeting SOCS3 and PIAS3, forming a positive feed-forward loop that drives carcinogenesis and tumor progression.

Cholangiocarcinoma is often difficult to diagnose at an early stage; accurate diagnosis frequently cannot be established until the disease is advanced and often in the metastatic stage, resulting in a poor prognosis. Given that the miR-17-92 cluster, particularly miR-92a, is highly expressed in cholangiocarcinoma, as shown in this study, further studies are needed to validate whether the miR-17-92 cluster or miR-92a can be used as a marker for early diagnosis of cholangiocarcinoma. Moreover, in light of the key role of miR-17-92 in cholangiocarcinogenesis and tumor progression, as described in the current study, further investigations are warranted to determine whether miR-17-92 can be targeted for the treatment of human cholangiocarcinoma.

Supplemental Data

Supplemental material for this article can be found at *http://dx.doi.org/10.1016/j.ajpath.2014.06.024*.

References

1. Filipowicz W, Bhattacharyya SN, Sonenberg N: Mechanisms of post-transcriptional regulation by microRNAs: are the answers in sight? Nat Rev Genet 2008, 9:102−114
2. Ambros V: The functions of animal microRNAs. Nature 2004, 431: 350−355
3. Lewis BP, Shih IH, Jones-Rhoades MW, Bartel DP, Burge CB: Prediction of mammalian microRNA targets. Cell 2003, 115:787−798
4. Lu J, Getz G, Miska EA, Alvarez-Saavedra E, Lamb J, Peck D, Sweet-Cordero A, Ebert BL, Mak RH, Ferrando AA, Downing JR, Jacks T, Horvitz HR, Golub TR: MicroRNA expression profiles classify human cancers. Nature 2005, 435:834−838
5. Calin GA, Sevignani C, Dumitru CD, Hyslop T, Noch E, Yendamuri S, Shimizu M, Rattan S, Bullrich F, Negrini M, Croce CM: Human microRNA genes are frequently located at fragile sites and genomic regions involved in cancers. Proc Natl Acad Sci U S A 2004, 101:2999−3004
6. Altuvia Y, Landgraf P, Lithwick G, Elefant N, Pfeffer S, Aravin A, Brownstein MJ, Tuschl T, Margalit H: Clustering and conservation patterns of human microRNAs. Nucleic Acids Res 2005, 33: 2697−2706
7. Yu J, Wang F, Yang GH, Wang FL, Ma YN, Du ZW, Zhang JW: Human microRNA clusters: genomic organization and expression profile in leukemia cell lines. Biochem Biophys Res Commun 2006, 349:59−68
8. Chaulk SG, Thede GL, Kent OA, Xu Z, Gesner EM, Veldhoen RA, Khanna SK, Goping IS, MacMillan AM, Mendell JT, Young HS, Fahlman RP, Glover JN: Role of pri-miRNA tertiary structure in miR-17∼92 miRNA biogenesis. RNA Biol 2011, 8:1105−1114
9. He L, Thomson JM, Hemann MT, Hernando-Monge E, Mu D, Goodson S, Powers S, Cordon-Cardo C, Lowe SW, Hannon GJ, Hammond SM: A microRNA polycistron as a potential human oncogene. Nature 2005, 435:828−833
10. Bonauer A, Dimmeler S: The microRNA-17-92 cluster: still a miRacle? Cell Cycle 2009, 8:3866−3873
11. Ota A, Tagawa H, Karnan S, Tsuzuki S, Karpas A, Kira S, Yoshida Y, Seto M: Identification and characterization of a novel gene, C13orf25, as a target for 13q31-q32 amplification in malignant lymphoma. Cancer Res 2004, 64:3087−3095
12. Hayashita Y, Osada H, Tatematsu Y, Yamada H, Yanagisawa K, Tomida S, Yatabe Y, Kawahara K, Sekido Y, Takahashi T: A polycistronic microRNA cluster, miR-17-92, is overexpressed in human lung cancers and enhances cell proliferation. Cancer Res 2005, 65:9628−9632
13. Tsuchida A, Ohno S, Wu W, Borjigin N, Fujita K, Aoki T, Ueda S, Takanashi M, Kuroda M: miR-92 is a key oncogenic component of the miR-17-92 cluster in colon cancer. Cancer Sci 2011, 102:2264−2271
14. Chow TF, Mankaruos M, Scorilas A, Youssef Y, Girgis A, Mossad S, Metias S, Rofael Y, Honey RJ, Stewart R, Pace KT, Yousef GM: The miR-17-92 cluster is over expressed in and has an oncogenic effect on renal cell carcinoma. J Urol 2010, 183:743−751
15. Si H, Sun X, Chen Y, Cao Y, Chen S, Wang H, Hu C: Circulating microRNA-92a and microRNA-21 as novel minimally invasive biomarkers for primary breast cancer. J Cancer Res Clin Oncol 2013, 139: 223−229
16. Liu GH, Zhou ZG, Chen R, Wang MJ, Zhou B, Li Y, Sun XF: Serum miR-21 and miR-92a as biomarkers in the diagnosis and prognosis of colorectal cancer. Tumour Biol 2013, 34:2175−2181
17. Shigoka M, Tsuchida A, Matsudo T, Nagakawa Y, Saito H, Suzuki Y, Aoki T, Murakami Y, Toyoda H, Kumada T, Bartenschlager R, Kato N, Ikeda M, Takashina T, Tanaka M, Suzuki R, Oikawa K, Takanashi M, Kuroda M: Deregulation of miR-92a expression is implicated in hepatocellular carcinoma development. Pathol Int 2010, 60:351−357
18. Rizvi S, Gores GJ: Pathogenesis, diagnosis, and management of cholangiocarcinoma. Gastroenterology 2013, 145:1215−1229
19. Patel T: Cholangiocarcinoma: controversies and challenges. Nat Rev Gastroenterol Hepatol 2011, 8:189−200
20. Fava G, Lorenzini I: Molecular pathogenesis of cholangiocarcinoma. Int J Hepatol 2012, 2012:630543
21. Tyson GL, El-Serag HB: Risk factors for cholangiocarcinoma. Hepatology 2011, 54:173−184
22. Sirica AE, Dumur CI, Campbell DJ, Almenara JA, Ogunwobi OO, Dewitt JL: Intrahepatic cholangiocarcinoma progression: prognostic factors and basic mechanisms. Clin Gastroenterol Hepatol 2009, 7: S68−S78
23. Park J, Tadlock L, Gores GJ, Patel T: Inhibition of interleukin 6-mediated mitogen-activated protein kinase activation attenuates growth of a cholangiocarcinoma cell line. Hepatology 1999, 30:1128−1133
24. Okada K, Shimizu Y, Nambu S, Higuchi K, Watanabe A: Interleukin-6 functions as an autocrine growth factor in a cholangiocarcinoma cell line. J Gastroenterol Hepatol 1994, 9:462−467
25. Meng F, Yamagiwa Y, Taffetani S, Han J, Patel T: IL-6 activates serum and glucocorticoid kinase via p38alpha mitogen-activated protein kinase pathway. Am J Physiol Cell Physiol 2005, 289: C971−C981
26. Meng F, Yamagiwa Y, Ueno Y, Patel T: Over-expression of interleukin-6 enhances cell survival and transformed cell growth in human malignant cholangiocytes. J Hepatol 2006, 44:1055−1065
27. Yamagiwa Y, Meng F, Patel T: Interleukin-6 decreases senescence and increases telomerase activity in malignant human cholangiocytes. Life Sci 2006, 78:2494−2502
28. Wehbe H, Henson R, Meng F, Mize-Berge J, Patel T: Interleukin-6 contributes to growth in cholangiocarcinoma cells by aberrant promoter methylation and gene expression. Cancer Res 2006, 66: 10517−10524
29. Isomoto H, Mott JL, Kobayashi S, Werneburg NW, Bronk SF, Haan S, Gores GJ: Sustained IL-6/STAT-3 signaling in cholangiocarcinoma cells due to SOCS-3 epigenetic silencing. Gastroenterology 2007, 132: 384−396

30. Goydos JS, Brumfield AM, Frezza E, Booth A, Lotze MT, Carty SE: Marked elevation of serum interleukin-6 in patients with cholangiocarcinoma: validation of utility as a clinical marker. Ann Surg 1998, 227:398–404
31. Tangkijvanich P, Thong-ngam D, Theamboonlers A, Hanvivatvong O, Kullavanijaya P, Poovorawan Y: Diagnostic role of serum interleukin 6 and CA 19-9 in patients with cholangiocarcinoma. Hepatogastroenterology 2004, 51:15–19
32. Cheon YK, Cho YD, Moon JH, Jang JY, Kim YS, Lee MS, Lee JS, Shim CS: Diagnostic utility of interleukin-6 (IL-6) for primary bile duct cancer and changes in serum IL-6 levels following photodynamic therapy. Am J Gastroenterol 2007, 102:2164–2170
33. Sansal I, Sellers WR: The biology and clinical relevance of the PTEN tumor suppressor pathway. J Clin Oncol 2004, 22:2954–2963
34. Alimonti A, Carracedo A, Clohessy JG, Trotman LC, Nardella C, Egia A, Salmena L, Sampieri K, Haveman WJ, Brogi E, Richardson AL, Zhang J, Pandolfi PP: Subtle variations in Pten dose determine cancer susceptibility. Nat Genet 2010, 42:454–458
35. Salmena L, Carracedo A, Pandolfi PP: Tenets of PTEN tumor suppression. Cell 2008, 133:403–414
36. Carracedo A, Alimonti A, Pandolfi PP: PTEN level in tumor suppression: how much is too little? Cancer Res 2011, 71:629–633
37. Xu X, Kobayashi S, Qiao W, Li C, Xiao C, Radaeva S, Stiles B, Wang RH, Ohara N, Yoshino T, LeRoith D, Torbenson MS, Gores GJ, Wu H, Gao B, Deng CX: Induction of intrahepatic cholangiocellular carcinoma by liver-specific disruption of Smad4 and Pten in mice. J Clin Invest 2006, 116:1843–1852
38. Chung JY, Hong SM, Choi BY, Cho H, Yu E, Hewitt SM: The expression of phospho-AKT, phospho-mTOR, and PTEN in extrahepatic cholangiocarcinoma. Clin Cancer Res 2009, 15:660–667
39. Adams EJ, Green JA, Clark AH, Youngson JH: Comparison of different scoring systems for immunohistochemical staining. J Clin Pathol 1999, 52:75–77
40. Olive V, Bennett MJ, Walker JC, Ma C, Jiang I, Cordon-Cardo C, Li QJ, Lowe SW, Hannon GJ, He L: miR-19 is a key oncogenic component of mir-17-92. Genes Dev 2009, 23:2839–2849
41. Malhi H, Gores GJ: Cholangiocarcinoma: modern advances in understanding a deadly old disease. J Hepatol 2006, 45:856–867
42. Zhao M, Sun J, Zhao Z: TSGene: a web resource for tumor suppressor genes. Nucleic Acids Res 2013, 41:D970–D976
43. Brock M, Trenkmann M, Gay RE, Gay S, Speich R, Huber LC: MicroRNA-18a enhances the interleukin-6-mediated production of the acute-phase proteins fibrinogen and haptoglobin in human hepatocytes. J Biol Chem 2011, 286:40142–40150
44. Brock M, Trenkmann M, Gay RE, Michel BA, Gay S, Fischler M, Ulrich S, Speich R, Huber LC: Interleukin-6 modulates the expression of the bone morphogenic protein receptor type II through a novel STAT3-microRNA cluster 17/92 pathway. Circ Res 2009, 104: 1184–1191
45. Schust J, Sperl B, Hollis A, Mayer TU, Berg T: Stattic: a small-molecule inhibitor of STAT3 activation and dimerization. Chem Biol 2006, 13:1235–1242
46. Collins AS, McCoy CE, Lloyd AT, O'Farrelly C, Stevenson NJ: miR-19a: an effective regulator of SOCS3 and enhancer of JAK-STAT signalling. PLoS One 2013, 8:e69090
47. Wu W, Takanashi M, Borjigin N, Ohno SI, Fujita K, Hoshino S, Osaka Y, Tsuchida A, Kuroda M: MicroRNA-18a modulates STAT3 activity through negative regulation of PIAS3 during gastric adenocarcinogenesis. Br J Cancer 2013, 108: 653–661